

RESEARCH ARTICLE

The Complete Genome Sequence of *Plodia interpunctella* Granulovirus: Evidence for Horizontal Gene Transfer and Discovery of an Unusual Inhibitor-of-Apoptosis Gene

Robert L. Harrison^{1*}, Daniel L. Rowley¹, C. Joel Funk²

1 Invasive Insect Biocontrol and Behavior Laboratory, Beltsville Agricultural Research Center, USDA Agricultural Research Service, Beltsville, Maryland, United States of America, **2** Department of Biology, John Brown University, Siloam Springs, Arkansas, United States of America

* Robert.L.Harrison@ars.usda.gov



OPEN ACCESS

Citation: Harrison RL, Rowley DL, Funk CJ (2016) The Complete Genome Sequence of *Plodia interpunctella* Granulovirus: Evidence for Horizontal Gene Transfer and Discovery of an Unusual Inhibitor-of-Apoptosis Gene. PLoS ONE 11(7): e0160389. doi:10.1371/journal.pone.0160389

Editor: Miguel Lopez-Ferber, Ecole des Mines d'Alès, FRANCE

Received: May 7, 2016

Accepted: July 18, 2016

Published: July 29, 2016

Copyright: This is an open access article, free of all copyright, and may be freely reproduced, distributed, transmitted, modified, built upon, or otherwise used by anyone for any lawful purpose. The work is made available under the [Creative Commons CC0](https://creativecommons.org/licenses/by/4.0/) public domain dedication.

Data Availability Statement: The nucleotide sequence data reported in this paper are available from GenBank (accession number KX151395).

Funding: This work was supported by funding from the National Institute of General Medical Sciences (<https://www.nigms.nih.gov/>), grant number P20 GM103429, awarded to C.J.F. The funders had no role in study design, data collection and analysis, decision to publish, or preparation of the manuscript.

Competing Interests: The authors have declared that no competing interests exist.

Abstract

The Indianmeal moth, *Plodia interpunctella* (Lepidoptera: Pyralidae), is a common pest of stored goods with a worldwide distribution. The complete genome sequence for a larval pathogen of this moth, the baculovirus *Plodia interpunctella* granulovirus (PiGV), was determined by next-generation sequencing. The PiGV genome was found to be 112,536 bp in length with a 44.2% G+C nucleotide distribution. A total of 123 open reading frames (ORFs) and seven homologous regions (*hrs*) were identified and annotated. Phylogenetic inference using concatenated alignments of 36 baculovirus core genes placed PiGV in the “b” clade of viruses from genus *Betabaculovirus* with a branch length suggesting that PiGV represents a distinct betabaculovirus species. In addition to the baculovirus core genes and orthologues of other genes found in other betabaculovirus genomes, the PiGV genome sequence contained orthologues of the bidensovirus NS3 gene, as well as ORFs that occur in alphabaculoviruses but not betabaculoviruses. While PiGV contained an orthologue of *inhibitor of apoptosis-5* (*iap-5*), an orthologue of *inhibitor of apoptosis-3* (*iap-3*) was not present. Instead, the PiGV sequence contained an ORF (PiGV ORF81) encoding an IAP homologue with sequence similarity to insect cellular IAPs, but not to viral IAPs. Phylogenetic analysis of baculovirus and insect IAP amino acid sequences suggested that the baculovirus IAP-3 genes and the PiGV ORF81 IAP homologue represent different lineages arising from more than one acquisition event. The presence of genes from other sources in the PiGV genome highlights the extent to which baculovirus gene content is shaped by horizontal gene transfer.

Introduction

Viruses of family *Baculoviridae* infect insects of orders Lepidoptera, Diptera, and Hymenoptera [1, 2]. These viruses are characterized as having relatively large (80–180 kbp), circular,

double-stranded DNA genomes that are packaged into rod-shaped, cylindrical capsids, which in turn are surrounded by a lipid envelope. Another key feature of these viruses is the formation of distinctive occlusion bodies consisting of a single highly-expressed viral protein (polyhedrin or granulin) assembled into a protective paracrystalline matrix around the enveloped virions.

Baculoviruses of genera *Alphabaculovirus* and *Betabaculovirus*, identified from moth and butterfly larvae, have received the most attention from researchers. Alphabaculovirus occlusion bodies (also referred to as polyhedra) are large polyhedral-shaped structures (0.15 to 15 μm) that contain multiple virions, often with >1 nucleocapsid per unit envelope [2]. Alphabaculoviruses, also known as nucleopolyhedroviruses (NPVs), can also productively infect insect cell lines derived from their hosts. This feature has facilitated much basic research on NPVs as well as the development of selected NPVs (such as *Autographa californica* multiple nucleopolyhedrovirus, or AcMNPV) into expression vectors [3]. Betabaculoviruses, also known as granuloviruses (GVs), differ by producing significantly smaller ovoid cylindrical occlusion bodies (approximately 0.13 x 0.5 μm) that contain a single virion [2]. There have been far fewer reports of successful infection of a cell line by a GV [4], and research with GV has lagged behind that of NPVs.

A granulovirus reported to infect larvae of the Indianmeal moth, *Plodia interpunctella*, was first described in 1968 [5]. Study of this virus, *Plodia interpunctella* granulovirus (PiGV), led to the creation and recognition of the species *Plodia interpunctella granulosis virus* (later renamed as *Plodia interpunctella granulovirus*) in family *Baculoviridae* in 1982 [6].

P. interpunctella is a prevalent and cosmopolitan pest of stored grains, nuts, and other dried foodstuffs. As a consequence, research on PiGV was carried out to evaluate it as a potential alternative to chemical insecticides for controlling infestations of *P. interpunctella* [7–10]. This research culminated in the registration of PiGV as a biopesticide [11]. PiGV was also the subject of study in early research on the molecular biology of baculovirus structural proteins and virion assembly [12–14]. Finally, PiGV and *P. interpunctella* have been developed into a model system for understanding the ecology and evolution of infectious disease, particularly with respect to factors affecting pathogen transmission [15–18], host susceptibility [19–22], host dynamics [23, 24], and response to infection [25–27].

As of this writing, complete or partial DNA sequence data for > 50 betabaculovirus isolates have been deposited in GenBank, including the open reading frame (ORF) of a PiGV chitinase gene (GenBank accession no. KP864638). To fully characterize the genome of PiGV, we isolated and sequenced genomic DNA isolated from PiGV granules. The complete PiGV genome sequence was determined, and analysis of this sequence suggests that the species *Plodia interpunctella granulovirus* is distinct from other species of *Betabaculovirus*. Our analysis highlighted the remarkable degree to which this virus has acquired genes from other sources.

Materials and Methods

Virus DNA isolation

PiGV stocks were obtained from the USDA-ARS Manhattan, KS laboratory where PiGV biopesticide and molecular biology research took place during the 1970s and 1980s [28, 29]. This PiGV isolate was obtained from D. K. Hunter (USDA-ARS, Fresno, CA) in 1972, and originated with the isolate characterized by Arnott and Smith [5]. The virus was propagated in *P. interpunctella* larvae, separated from cell debris using a sucrose cushion, then purified using sucrose gradients [30]. Purified PiGV granules were solubilized in 0.1 M sodium carbonate and DNA was extracted from occluded virus as previously described [31, 32].

Genome sequencing and assembly

Genomic DNA was sequenced as previously described [32] except that the DNA was fragmented and the MID tags added at University of Florida Interdisciplinary Center for Biotechnology Research (Gainesville, FL). Sequencing reads from a Roche 454 GS Junior instrument were sorted and assembled using the SeqMan NGEN V3.0 assembler program (Lasergene; DNASTAR, Inc., Madison, WI) with default parameters. PCR and Sanger dideoxy sequencing were carried out to close gaps in the alignment and resolve or confirm regions with ambiguous sequences or unusual features, including 17 N₈₊ homopolymer regions. The Lasergene SeqManPro (version 12) sequence editor was used to prepare the final contig of the consensus genome sequence. The PiGV genome sequence generated for this study has been deposited in GenBank with the accession number KX151395.

ORF and homologous repeat region (*hr*) annotation

ORFs identified in the PiGV genome sequence were annotated if they were >50 codons in length and were evolutionarily conserved with other viral or non-viral ORFs, as ascertained by BLASTp. ORFs which did not yield a significant match by BLASTp (e.g. no matches with e-values <0.010) were annotated if they did not overlap a larger ORF by >75 bp and if they were predicted to be protein-encoding by both the fgenesV (<http://linux1.softberry.com/berry.phtml>) and ZCURVE_V [33] algorithms. In accordance with the convention for numbering baculovirus ORFs, the ORF encoding granulins was designated as ORF1, and the adenine of the granulins ORF start codon was designated as nt 1 of the genome.

Homologous region (*hr*) sequences were identified using the pattern- and repeat-finding functions of the LaserGene GeneQuest program (DNASTAR), Tandem Repeats Finder [34], and REPuter [35]. Individual repeats from the *hrs* were aligned using Clustal W in LaserGene MegAlign (DNASTAR), and the alignment and repeat consensus sequence were displayed with BOXSHADE (http://www.ch.embnet.org/software/BOX_form.html).

Sequence comparison and phylogeny

Shared synteny between PiGV and *Plutella xylostella* granulovirus K1 (PlxyGV-K1) [36], *Cydia pomonella* granulovirus isolate M1 (CpGV-M1; [37], and *Pieris rapae* granulovirus isolate Wuhan (PiraGV-Wuhan; [38] was determined by constructing gene parity plots [39].

To identify genetic differences between the PiGV genome reported in this study and the PiGV transcriptome sequences reported by [40], pairwise alignment was carried out between the PiGV genome sequence and the PiGV transcriptome contigs located at <http://afterparty.bio.ed.ac.uk/study/show/2194070> [40].

The relationship of PiGV to other baculoviruses was inferred from the concatenated alignments of 36 of 37 putative baculovirus core genes [41]. An alignment of P6.9 amino acid sequences was not included in the analysis, as ORF31 of the gammabaculovirus *Neodiprion abietis* nucleopolyhedrovirus (NeabNPV) does not encode a *p6.9* homologue and no complete *p6.9* ORF has not been identified in the NeabNPV genome. In addition, the homologue of the *ac78* core gene in NeabNPV is not ORF46 as reported by Garavaglia et al., but is instead an unannotated ORF extending from nt 42344←42628 in the NeabNPV genome. The amino acid sequence specified by this unannotated ORF was used in the AC78 alignment. The baculovirus core gene amino acid alignments were concatenated using BioEdit 7.1.3 [42].

In addition, amino acid sequence alignments were assembled with additional individual PiGV ORFs of interest (PiGV ORF11, ORF15, ORF18, and ORF81) and related viral and non-viral homologues of these ORFs.

In all cases, amino acid sequences were aligned by Clustal W using LaserGene MegAlign (DNASTAR) with default parameters, except for desmoplakin (AC66), AC78, PiGV ORF15, ORF18, and ORF81. For these alignments, the multiple and pairwise alignment penalties were reduced from 10 to 5 and the multiple alignment gap length penalty was reduced from 0.2 to 0.1 to compensate for the lower degree of conservation among the sequences of these proteins. Phylogenetic trees were constructed with the minimum evolution (ME) method using MEGA6 [43] with 500 bootstrap replicates. A phylogenetic tree was also inferred from the same alignment by maximum likelihood using either MEGA6 (for the individual PiGV ORF alignments) or RAxML 7.7.1 [44] (for the concatenated core gene alignment). MEGA6 was used to identify the best-fitting evolutionary models to use with these analyses and to calculate the gamma shape parameter for site rate differences.

The sequences used for phylogenetic inference are listed in [S1 Table](#).

Results and Discussion

Properties of the PiGV genome

Assembly of 454 and Sanger dideoxy sequencing data yielded a genome of 112,536 bp with a coverage of 53.9 X ([Fig 1](#)). The size is lower than the mean GV genome size of 123,464 (n = 18), though this average is skewed by the inclusion of the unusually large *Helicoverpa armigera* GV (HearGV) and *Xestia c-nigrum* GV (XecnGV) genomes [45, 46]. The PiGV genome is closest in size to that of *Cryptophebia leucotreta* GV (CrleGV), which is 110,907 bp [47]. The PiGV nucleotide distribution, at 44.2% G+C, is closest to that of *Clostera anachoreta* granulovirus-HBHN (ClanGV-HBHN; [48]) at 44.4% G+C. Up to 123 ORFs were annotated for the PiGV genome, with 64 in the sense direction and 59 in the antisense direction ([Fig 1](#), [S2 Table](#)).

Seven homologous repeat regions (*hrs*) were identified in the PiGV genome. These *hrs* consist of 1–3 imperfect palindromes ranging in size from 49 to 83 bp and bound by inverted repeats with the consensus sequence TGATGACGAA ([Fig 2](#)). The consensus sequence of the PiGV *hr* terminal repeats did not closely match the consensus terminal sequence found to be conserved among the *hrs* of five GVs [49]. However, six of the seven PiGV *hrs* are located in positions that are conserved among other GV genomes for *hrs*, such as next to CpGV ORF *cp5* (*hr1*), between *sod* and *p74* (*hr3*), upstream of *p47* (*hr4*), within *vp91* (*hr5*), next to *dna ligase* (*hr6*), and within *lef-8* (*hr7*) [45]; [Fig 1](#), [S2 Table](#)). Some *hrs* of CpGV and CrleGV have been found to act as origins of DNA replication in *C. pomonella* tissue culture-based assays [49, 50], and it seems likely that PiGV *hrs* perform the same function in PiGV-infected *P. interpunctella* cells.

Relationships to other baculoviruses

Blastp queries with the conceptual amino acid sequences of PiGV ORFs yielded the highest-scoring matches with ORFs from a wide variety of betabaculoviruses, including isolates of CpGV, CrleGV, *Agrotis segetum* granulovirus (AgseGV), *Choristoneura occidentalis* granulovirus (ChocGV), *Clostera anastomosis* granulovirus-A (ClanGV-A, or CaLGV) and -B (ClanGV-B), *Lacanobia oleracea* granulovirus (LaolGV), *Pieris rapae* granulovirus (PiraGV), *Phthorimaea operculella* granulovirus (PhopGV), *Epinotia aporema* granulovirus (EpapGV), *Erinnyis ello* granulovirus (ErelGV), *Spodoptera frugiperda* granulovirus (SpfrGV), and *Spodoptera litura* granulovirus (SpltGV) ([S2 Table](#)). PiGV ORF1, encoding granulin, was the most conserved gene, exhibiting a 94.4% amino acid sequence similarity with the encoded granulin of CrleGV. Other ORFs encoding granulovirus homologues exhibited amino acid similarities

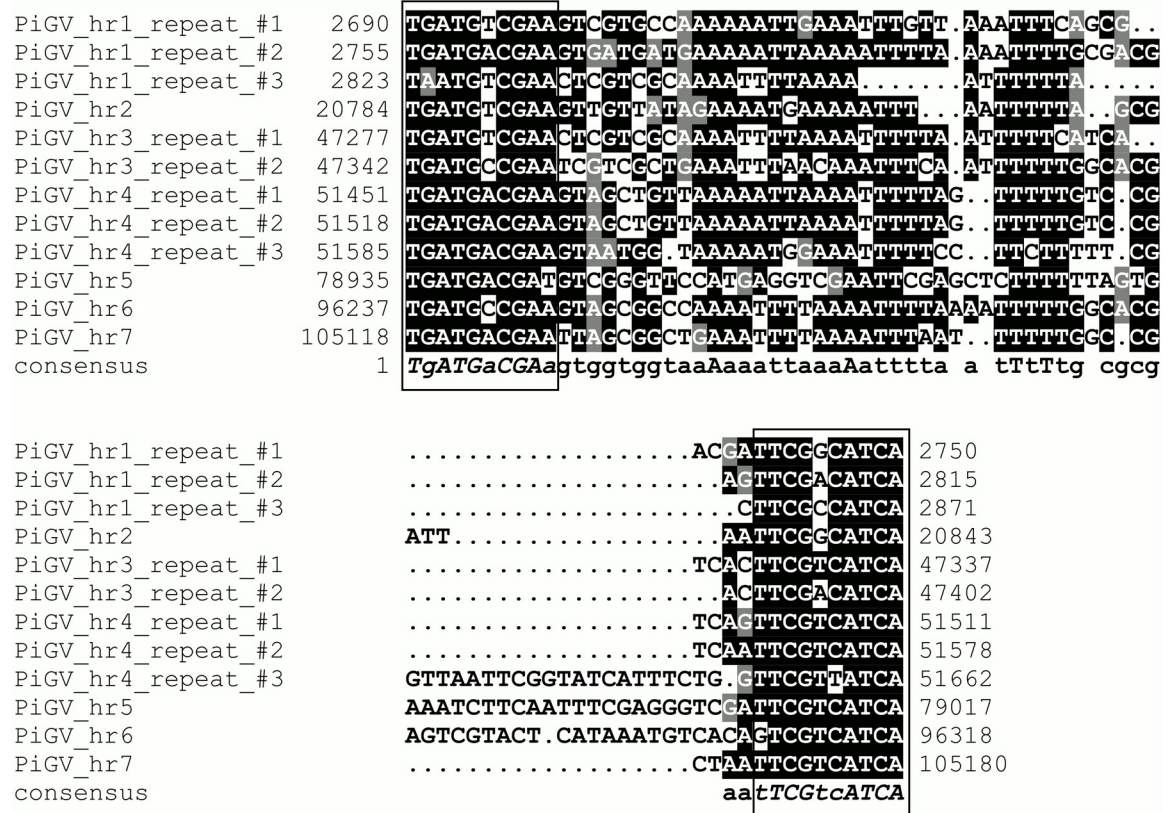


Fig 2. Alignment of PiGV homologous region (hr) palindromic repeats. Nucleotide positions of the repeats in the genome sequence are indicated. Identical nucleotides occupying >50% of aligned positions are shaded in black, and nucleotides of the same class as conserved nucleotides (containing either a purine or pyrimidine base) are shaded in gray. Nucleotides in the repeat consensus sequence are denoted by uppercase letters for positions in the alignment with completely identical residues, and lowercase letters for positions in the alignment with a majority of identical residues. The conserved 10-bp inverted terminal repeat sequence is indicated by boxes surrounding the aligned sequence at each end.

doi:10.1371/journal.pone.0160389.g002

from other clade b sequences by long branch lengths and does not appear to be closely related to any particular GV.

Gene parity plot analysis was carried out to visualize the synteny between the genomes of PiGV and two other clade b granuloviruses (CpGV-M1 and PiraGV-Wuhan). Gene order in the PiGV genome was also compared with that of a clade a granulovirus that has a genome of a comparable size (PlxyGV; 100,999 bp). Although the gene content differences between PiGV and PlxyGV were visibly more numerous than those between PiGV and the clade b GVs, the degree of synteny was not noticeably different (Fig 4).

Recently, the transcriptome of *P. interpunctella* larvae infected with PiGV and harvested at 24 hours post-infection (hr p. i.) was reported [40]. The authors of this study identified contigs of granulovirus origin (ascertained by BLAST alignment with the sequence of PlxyGV) and concluded that they had assembled viral sequence data from the infected *P. interpunctella* transcriptome amounting to an estimated 44% of the PiGV genome. Comparison of the PiGV genome with the viral contigs assembled from transcriptomic data [40] revealed that the virus used by McTaggart and co-workers is the same virus reported here. Transcriptome reads from this project assembled into eleven contigs that aligned with PiGV nt 2841–7436, 10664–13710, 18056–27589, 29803–34735, 64189–69653, 70348–71408, 72086–77471, and 79003–96283, for a total of 51, 303 bp or 45.6% of the genome. Two of the transcriptome contigs consist of an

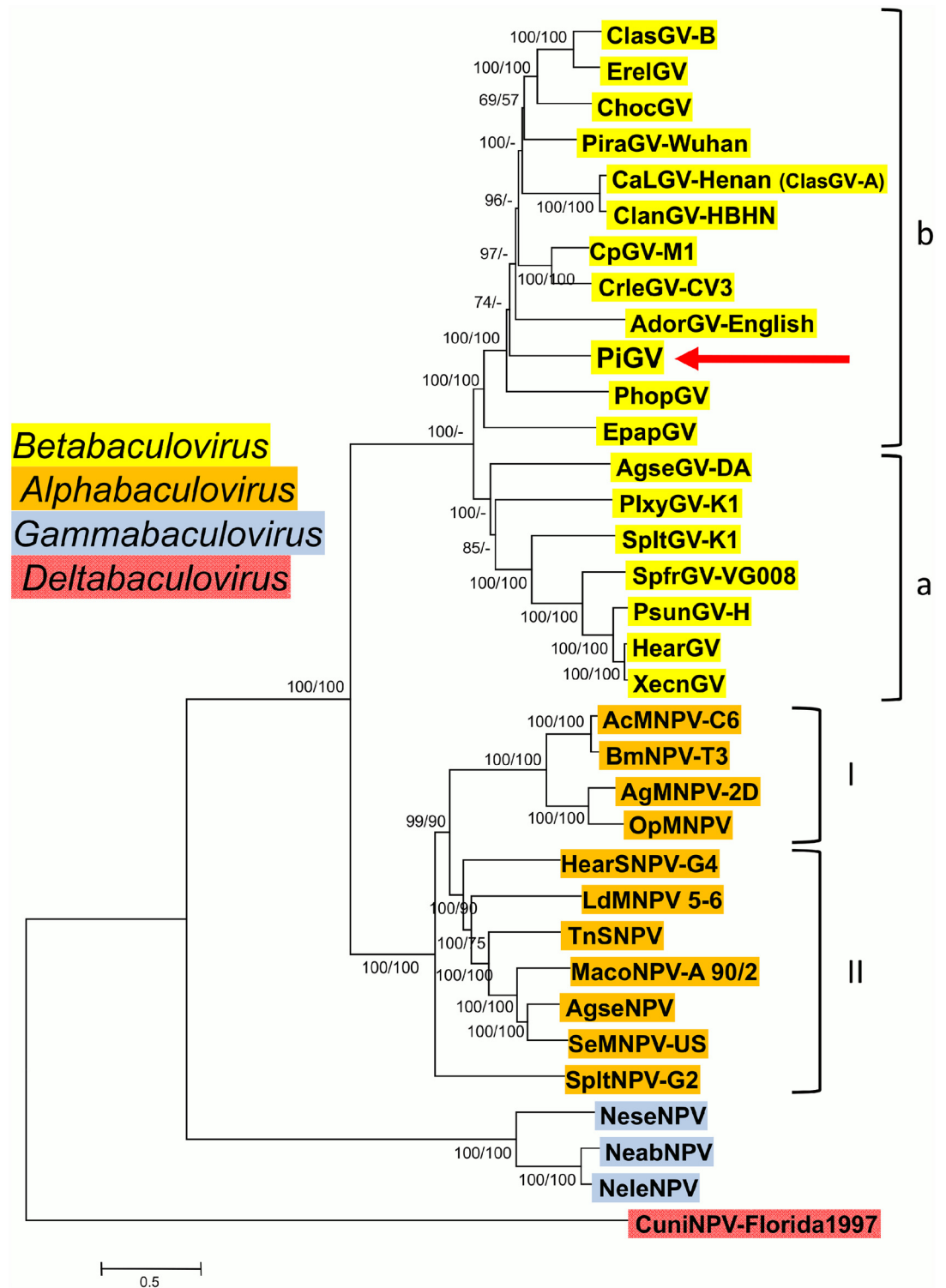


Fig 3. Relationships of PiGV and representative isolates of other baculovirus species, inferred from the predicted amino acid sequences of baculovirus core genes. The phylogenetic tree was constructed from the concatenated alignments of 36 baculovirus core gene amino acid sequences using the minimum-evolution (ME) method. Taxon genera are indicated with colored text background. Both the group I and II clades of genus *Alphabaculovirus* and the a and b clades of *Betabaculovirus* are indicated with brackets. Bootstrap values >50% for both ME and maximum likelihood (ML) analysis are indicated for each interior branch (ME/ML). In addition to PiGV (indicated by a red arrow), virus taxa and accession numbers used in the analysis are as indicated in [S1 Table](#).

doi:10.1371/journal.pone.0160389.g003

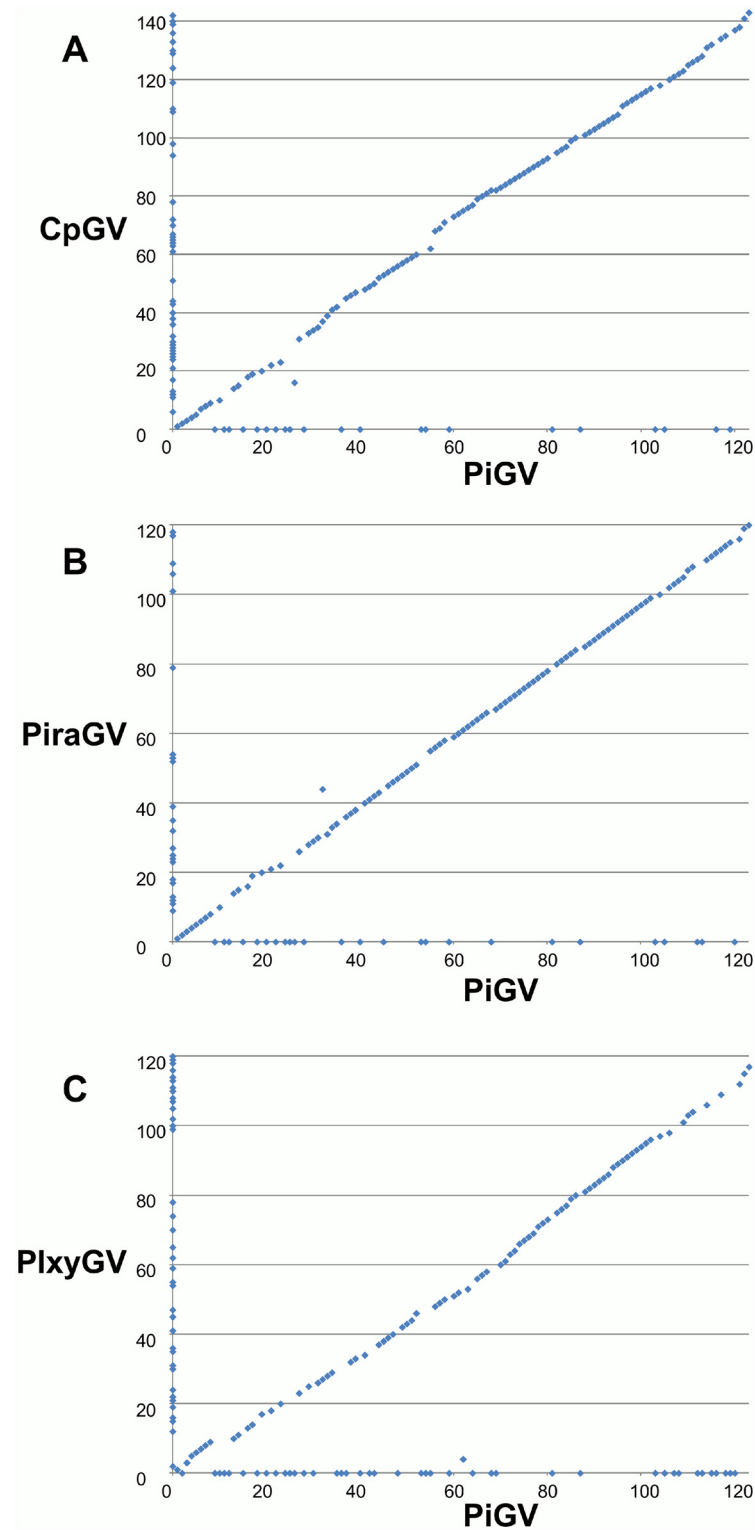


Fig 4. Gene parity plots comparing PiGV with representative clade a and b granuloviruses. Plots show the ORF content and order of the PiGV genome (x-axis) with that of (A) CpGV, (B) PiraGV, and (C) PlxyGV (y-axes). Each point in the plot represents an ORF. ORFs present in only one of the compared genomes appear on the axis corresponding to the virus in which they are present.

doi:10.1371/journal.pone.0160389.g004

inverted repeat of the same sequence—for example, nt 1→4891 of contig comp66738_c0_seq1 aligns with the antisense strand of PiGV genome nt 88851←93740, while nt 4808→9698 of the same contig aligns with the sense strand of the same region of PiGV (nt 88851→93740). PCR with PiGV genomic DNA and primers that annealed close to the inversion points in these contigs failed to produce amplicons, indicating that the inversions in these contigs were the result of erroneous assembly. These contigs may have led McTaggart and co-workers to conclude that there were inversions of the PiGV genome sequence relative to that of PlxyGV in a dot-plot of the PiGV-derived sequence vs. the PlxyGV genome sequence, [40]. Our gene parity plot analysis does not support the presence of large-scale inversions in the PiGV genome relative to the genome of PlxyGV.

Alignment of the consensus PiGV genome and the McTaggart et al. viral transcriptomic sequences revealed a total of 66 substitutions (28 synonymous, 26 nonsynonymous, and 12 intergenic), for a rate of 1.3 substitutions/kbp (Table 1). In addition, 23 indels (12 intergenic and 11 located within ORFs) were detected. Thirty-six of the substitutions and six of the indels in Table 1 also were found in a minority of the 454 genome sequence reads, ranging in frequency from 10% (indel at nt 12508) to 48.8% (C to T substitution at nt 90715) with an average frequency of 27.9%. Of the 11 indels in ORFs, 10 of them were in-frame and 1 resulted in a frameshift within PiGV ORF14. This ORF is an orthologue of *p49* (AcMNPV ORF *ac142*), which appears to be required for virus production [52, 53]. The indel in *p49*, which increases a homopolymer repeat from A₈ to A₉, is present in 10% of the 454 genome sequence reads, suggesting that it corresponds to a minor genotype that may be dependent on P49 supplied in *trans*.

Gene content

The PiGV genome contained all 37 of the core genes proposed for *Baculoviridae* by Garavaglia et al. [41] (Fig 1). Several non-core genes conserved among all members of *Alphabaculovirus* and *Betabaculovirus* were also found in the PiGV genome, including *granulin*, *pk-1*, *ac13*, *ac23*, *dbp*, *lef-6*, *ubiquitin*, *pp31*, *lef-11*, *ac38*, *fp25k*, *lef-3*, *ac75*, *tlp*, *p12*, *ac106/107*, *ac108*, *ac110*, *p24*, *pep*, *me53*, *ac145*, *ac146*, and *ie-1*. Two genes claimed by Garavaglia et al. to be conserved among betabaculoviruses, *gp37* and *exon0*, were not found in PiGV. These genes also do not occur in the genomes of SpfrGV-VG008, ErelGV, or in isolates of AgseGV.

The remaining ORFs in the PiGV genome consist of (a) ORFs with homologues among granuloviruses (S2 Table) and (b) ORFs with no granulovirus homologues (Table 2). Among the former class of ORFs is PiGV ORF11, which had the most significant blastp match with an ORF from isolates of *Bombyx mori bidensovirus*, the sole species of the recently-created virus family *Bidnaviridae* [54]. Other homologues have been described from a handful of granulovirus genomes, including those of CrleGV-CV3, ChocGV, Clostera anastomosis granulovirus B (ClasGV-B), and ErelGV. A homologue has also been identified in the genome of *Perigonia lusca* single nucleopolyhedrovirus (PelusNPV). The encoded amino acid sequences of these genes also share similarity with amino acid sequences of the NS3 gene found in isolates of the densovirus species *Lepidopteran ambidensovirus 1*. Phylogenetic inference of these sequences grouped the densovirus sequences together as well as the two copies of the homologue found in ErelGV with strong bootstrap support (Fig 5). PiGV ORF11 was grouped with the bidensovirus sequences, and homologues from ClasGV-B and PelusNPV were grouped together with moderate bootstrap support, while there was no significant bootstrap support for the positions of the other homologues. From the phylogeny, it appears that homologues of the densovirus/bidensovirus NS3 sequences appeared in baculovirus genomes as a result of independent acquisition events. This conclusion is consistent with that drawn by Ardisson-Araújo et al. [55] from

Table 1. Genetic variation between the consensus PiGV genome sequence and *P. interpunctella* transcriptome sequences of viral origin reported by McTaggart et al. [40].

Substitution or indel ^a	Gene or region affected
A5697G	Chitinase (ORF10); synonymous substitution
G11428A ; G11902T; G12346A (A) inserted after 12508 (8A->9A)	<i>p49</i> (ORF14); frameshift in 7 th codon, 2 synonymous substitutions and 1 non-synonymous substitutions occurring downstream.
Δ12640–12750; Δ12790–12792	Between ORF14 and ORF15
T13000C ; G13487A; A13624G	ORF15; 3 synonymous substitutions
Δ18562–18635; Δ18777 (4T->3T)	Between ORF20 and ORF21
C18910A; C19166A; G19216A; A19248G; A19307G ; (GGT) inserted after 19336 ; A19367G ; (CTTCAGACG) inserted after 19495	<i>pep-p10</i> (ORF21); 4 nonsynonymous substitutions, 2 synonymous substitutions, 1 3 nt insertion, 1 9 nt insertion
Δ19809; T19960G ; T19963G	Between ORF21 and ORF22
Δ20106–20114	ORF22; 1 9-nt deletion
A21721T	ORF24; nonsynonymous substitution
T22038C; Δ22215–22224 ; Δ22250; Δ22412; A22788G	Between ORF24 and ORF25
Δ23361–23363; G23412A; (AACTTTCCAGCT) inserted after 23523 ; (CGTCGACGAGCC) inserted after 23594; A23649G; Δ23669–23692 A23708G; T23738A; (AAAAAG) inserted after 23786	ORF25; 1 3-nt deletion, 1 24-nt deletion, 2 12-nt insertions, 1 6-nt insertion, 2 nonsynonymous substitutions, 2 synonymous substitutions
Δ24679 (9A to 8A); (T) inserted after 24699 (9T to 10T)	Between ORF25 and ORF26
C25274T	<i>nrk-1</i> (ORF26); nonsynonymous substitution
C27052T	<i>efp</i> (ORF27); synonymous substitution
C30502T	ORF30; synonymous substitution
C31352T	<i>pif-3</i> (ORF31); synonymous substitution
G31427A ; G31440A ; G32000T; G32183A; C32591T; Δ33295–33357	<i>odv-e66</i> (ORF32); 1 63-nt deletion, 3 nonsynonymous substitutions, 2 synonymous substitutions
C33677T	ORF33; 1 synonymous substitution
G33929A; A33939G	Between ORF33 and ORF34
A34556G ; T34578C ; A34579C ; G34689T	ORF35; 3 nonsynonymous substitutions and 1 synonymous substitution
C64930T ; G65260C	<i>38k</i> (ORF75); 2 synonymous substitutions
C68357T	<i>helicase</i> (ORF77); 1 synonymous substitution
A72799G	ORF81; 1 nonsynonymous substitution
A73652G ; T73660G	<i>lef-4</i> (ORF82); 1 synonymous and 1 nonsynonymous substitutions
Δ76289–76310	ORF85; 1 22-nt deletion of a repeated sequence at the 3' end of the ORF-no impact on encoded amino acid sequence.
A77453C	ORF86; 1 synonymous substitution
C79226T; G79375A	Between <i>hr5</i> and ORF89
A80342G	ORF90; 1 nonsynonymous substitution
T82426A ; G82575A	<i>vlf-1</i> (ORF93); 1 synonymous and 1 nonsynonymous substitutions
G83369A	ORF95; 1 nonsynonymous substitution
A86263G	<i>dnapol</i> (ORF96); 1 synonymous substitution
A86772G ; A87134G ; C88503A; C88667A	<i>desmoplakin</i> (ORF97); 1 synonymous and 3 nonsynonymous substitutions
T88858C; T88861C	Between <i>desmoplakin</i> and <i>lef-3</i>

(Continued)

Table 1. (Continued)

Substitution or indel ^a	Gene or region affected
G89257A	<i>lef-3</i> (ORF98); 1 synonymous substitution
C90715T	ORF100; 1 synonymous substitution
T91296C	<i>iap-5</i> (ORF101); 1 synonymous substitution
G92715A; G92800A; C92804A; C93097A	<i>lef-9</i> (ORF102); 1 synonymous and 3 nonsynonymous substitutions
(T) inserted after 93363 (6T to 7T)	Between ORF102 and ORF103
Δ96280 (5T to 4T)	<i>hr6</i>

^aNucleotide positions in the genome sequence are indicated. For substitutions, the nucleotide identity in the genome followed by the nucleotide position and the nucleotide identity in the associated transcriptomic contig. Deletions (Δ) and insertions are described in relation to the consensus genome sequence. Indels and substitutions in bold italics also are present in a minority of the genome sequence 454 reads.

doi:10.1371/journal.pone.0160389.t001

their analysis of a smaller data set. An alternative hypothesis for the presence of NS3 homologues in the betabaculovirus genomes involves a single ancient acquisition event followed by sequence divergence. The NS3 homologue in PeluSNPV may be due to horizontal gene transmission from a granulovirus, or it may point to an NS3 gene acquisition that predated the divergence of alphabaculoviruses and betabaculoviruses. In either case, for this hypothesis, one would also have to stipulate that the NS3 gene was subsequently lost from most baculovirus lineages. With regard to the possible functional significance of these genes, Junonia coenia densovirus NS3 was shown to be required for viral DNA replication [56], while BmDENV-Zhenjiang NS3 was shown to interact with a transgelin homologue and a serine protein precursor in *B. mori* BmN cells [57]. It is unclear what role, if any, the baculovirus homologues of these genes possess in the baculovirus life cycle.

Table 2. PiGV ORFs with no orthologues in other granulovirus genomes.

ORF	Position/Size (aa)	Best blastp match	Notes
9 (<i>dut</i>)	5169→5594/141	Bathycoccus sp. RCC1105 virus BpV1 dUTPase; 42.6% (60/141)	Blastp match with a single baculovirus <i>dut</i> (<i>Spodoptera frugiperda</i> MNPV); no blastp matches to other GV <i>dut</i> genes
12	8421←10262/613	-	No conserved domains
15 (<i>ac11</i>)	12857←13942/361	Choristoneura fumiferana DEF MNPV ORF9; 21.7% (80/368)	
18 (<i>ac11</i>)	15613→16524/303	Bombyx mori NPV-T3 ORF4; 40.4% (130/322)	
22	19988→20560/190	-	No conserved domains
24	20934←21959/341	-	No conserved domains
25	22903→24189/428	-	No conserved domains
28	27464→29122/552	-	Contains SMC_prok_B domain
36	34788←35198/136	-	No conserved domains
40	38516←39430/304	-	No conserved domains
53	49474→50136/330	-	No conserved domains
54	50237→51379/380	-	No conserved domains
81	71674←72873/399	GM24450 [<i>Drosophila sechellia</i>]; 30.9% (131/424)	Inhibitor of apoptosis (IAP), with 2 BIR and 1 RING finger domains
87	77672←77974/100	mucin-2-like [<i>Amyeloid transitella</i>]; 50.0% (34/68)	Many matches with mucin-2 and mucin-2-like sequences; contains ChtBD2 (chitin-binding) domain
103	93414→93659/81	Lymantria dispar MNPV-27 ORF25; 44.3% (35/79)	
105	94221←94562/113	-	No conserved domains

doi:10.1371/journal.pone.0160389.t002

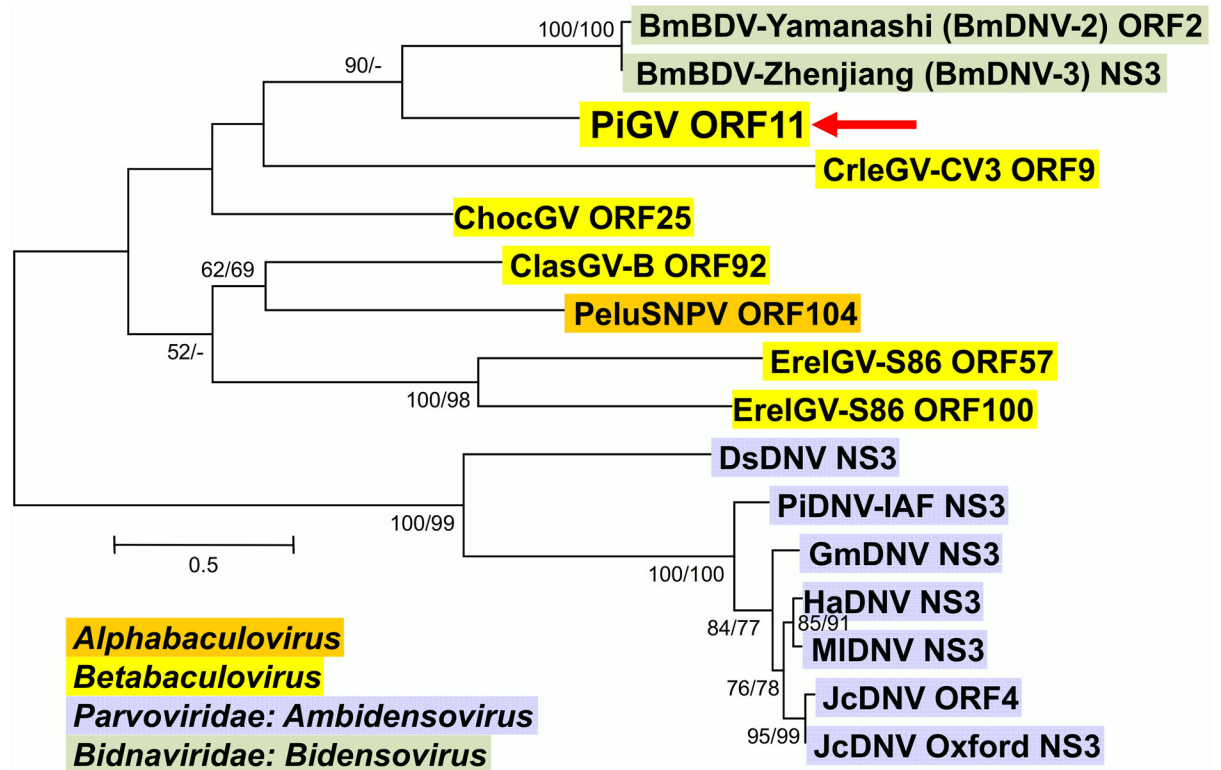


Fig 5. Phylogenetic analysis of baculovirus, bidensovirus, and densovirus NS3 homologues. ME phylogram inferred from the alignment of NS3 homologue amino acid sequences are shown with bootstrap values (>50%) at interior branches for ME and ML analysis (ME/ML) where they occur. In addition to PiGV (indicated by a red arrow), virus taxa are as indicated in S1 Table. Family and/or genus of each taxon is indicated with a color-coded text background.

doi:10.1371/journal.pone.0160389.g005

ORFs with alphabaculovirus homologues. Four PiGV ORFs—ORF9, ORF15, ORF18, and ORF103—encode sequences that only exhibit significant sequence similarity to alphabaculovirus ORFs.

ORF9 encodes an amino acid sequence with significant similarity to dUTPases (*dut*) from a number of sources. Although the granuloviruses AgseGV, EpapGV, ErelGV, and SpfrGV-VG008 also encode *dut* homologues, none of these GV dUTPase sequences appeared in a BLASTp search with PiGV ORF9 as a query sequence. The only baculovirus homologue that appeared as a match to ORF9 by blastp was that of Spodoptera frugiperda multiple nucleopolyhedrovirus (SfMNPV). This result suggests that the *dut* homologues in the PiGV genome and other GV genomes are a consequence of a separate gene acquisition events. Recent comprehensive analyses of baculovirus *dut* gene phylogeny [58, 59] supports this hypothesis, in one case finding that the *dut* genes present in baculovirus genomes are the product of at least nine horizontal gene transfer events [59].

Both ORF15 and ORF18 encode homologues of the AcMNPV ORF *ac11*. Homologues of this gene have only been found in all group I alphabaculoviruses and a selection of group II alphabaculoviruses. Phylogenetic inference of relationships among *ac11* homologues points to two well-supported clades of group I alphabaculovirus sequences (Fig 6). The homologues from PiGV and the group II alphabaculoviruses occur outside these clades and are separated by long branch lengths, suggesting that these homologues have diverged extensively from each other and/or are the results of horizontal gene transfer. ORF15 and ORF18, which only share

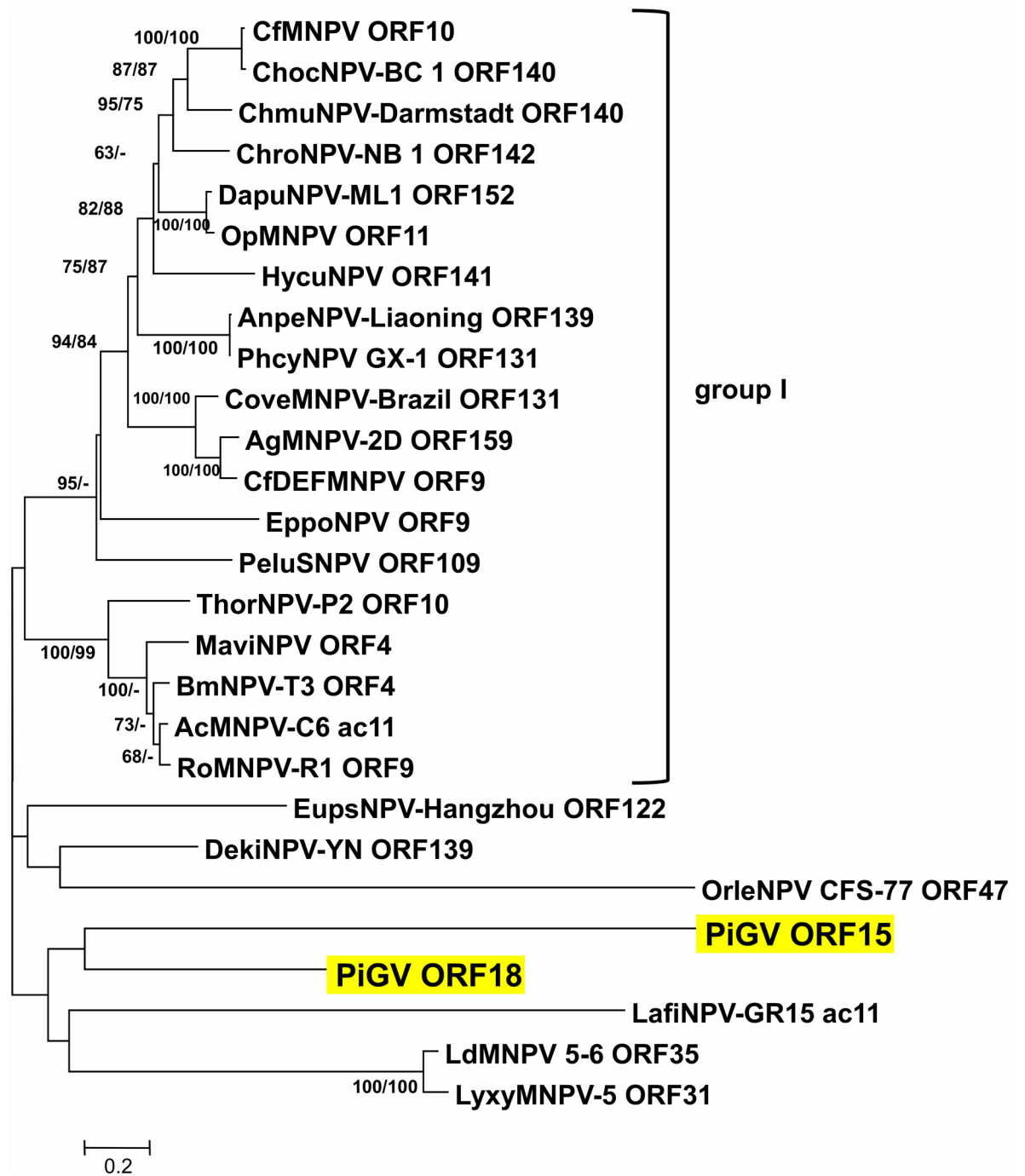


Fig 6. Phylogenetic analysis of baculovirus *ac11* homologues. ME phylogram inferred from the alignment of AcMNPV *ac11* homologue amino acid sequences are shown with bootstrap values (>50%) at interior branches for ME and ML analysis (ME/ML) where they occur. Virus taxa and accession numbers used in the analysis are as indicated in S1 Table. The PiGV *ac11* homologues are highlighted in yellow, and the group I alphabaculovirus sequences are indicated by a bracket.

doi:10.1371/journal.pone.0160389.g006

26% amino acid sequence identity with each other, are grouped together but with no significant degree of support. Two homologues of the same gene in the same genome could arise from a single acquisition event followed by gene duplication and sequence divergence. However, given the degree of sequence divergence between the ORF15 and ORF18 sequences, and in the

absence of reports of *ac11* homologues in other granulovirus genomes, it seems more likely that ORF15 and ORF18 resulted from independent acquisition events. In cells infected with an AcMNPV *ac11* knockout mutant bacmid-generated virus, both nucleocapsid egress from the nucleus and intranuclear envelopment of nucleocapsids were absent, suggesting an essential role for *ac11* in those particular steps in virion morphogenesis [60]. It is unclear if the PiGV homologues play a similar role in PiGV-infected cells.

Finally PiGV ORF103 encodes a homologue of an ORF annotated in isolates of *Lymantria dispar* multiple nucleopolyhedrovirus (LdMNPV), *Lymantria xyli* nucleopolyhedrovirus (LyxyNPV), and isolates of the nudivirus species *Heliothis zea nudivirus*. Although the annotation for the LdMNPV 5–6 isolate genome indicates that this is a homologue of AcMNPV *ac4* [61], blastp and HMMER [62] queries with PiGV ORF103 and the LdMNPV orthologue sequences did not yield matches with *ac4* or any other baculovirus gene.

ORFs encoding inhibitor of apoptosis (IAP) homologues. Inhibitors of apoptosis (IAPs) are functionally diverse proteins that were originally identified in baculoviruses as inhibitors of host cell apoptosis [63–67]. They were subsequently found in both eukaryotic organisms and in other DNA viruses. IAPs are recognized by the presence of at least one baculoviral IAP repeat (BIR) domain, which mediates protein interaction. Baculovirus IAPs also contain a copy of a Really Interesting New Gene (RING) domain in the C-terminus.

Clem (2015) [67] identified 6 distinct groups of IAP-encoding genes found in baculovirus genomes. The genes *iap-1*, *iap-2*, and *iap-4* have been found only in alphabaculoviruses, while *iap-5* and *iap-6* genes are found exclusively in betabaculoviruses. Genes of the *iap-3* group are found among alphabaculoviruses, betabaculoviruses, and gammabaculoviruses.

In the PiGV genome, ORF101 was identified as an *iap-5* orthologue. However, no orthologue for *iap-3* or *iap-6* was found. Instead, a second *iap* homologue encoded by PiGV ORF81 was identified that did not appear to correspond to any of the baculovirus *iap* groups described by Clem (2015) [67]. A blastp query with the ORF81 amino acid sequence yielded 189 matching sequences that included mostly IAP sequences from insects of orders Diptera (flies and mosquitoes), Hymenoptera (ants and wasps), Hemiptera (true bugs), with additional matches with a few sequences from Coleoptera (beetles), Isoptera (termites), and Dictyoptera (cockroaches). No baculovirus IAP sequences were among these matches, and only one IAP sequence from a moth, *Galleria mellonella* (order Lepidoptera; Genbank accession no. ACV04797, expected value of $2e^{-13}$), occurred in the results of the query. *G. mellonella*, like *P. interpunctella*, is classified in the family Pyralidae. A tBlastn search of the McTaggart et al. [40] *P. interpunctella* transcriptome contigs with the sequences of the *G. mellonella* IAP and an IAP from the pyralid moth *Amyelois transitella* (Genbank accession no. XP_013192077) failed to yield any matches. A search of the annotation for these contigs also failed to find any sequences identified as encoding inhibitors of apoptosis in the *P. interpunctella* transcriptome.

An examination of the ORF81 amino acid sequence revealed the existence of two BIR motifs and a C-terminal RING domain (Fig 7). ORF81 is thus similar to baculovirus IAP-1, IAP-3, and IAP-5, which also possess two BIRs and one RING domain. However, at 399 amino acids, the protein encoded by ORF81 was significantly larger than those encoded by baculovirus *iap* genes (which range from approximately 240–310 amino acids). Rather, the size of the ORF81 protein was more similar to that of insect cellular IAP homologues (Fig 7). Cellular insect IAPs possess an N-terminal leader sequence occurring prior to the first BIR repeat (BIR1) that is longer than the sequence upstream of BIR1 in baculovirus IAPs (Fig 7). In lepidopteran IAPs, leader sequence contains a mitogen-activated kinase (MAPK) degron motif (TPxxS) which mediates the turnover of cellular IAPs in baculovirus-infected cells [68]. The PiGV ORF81 protein does not possess an extended leader sequence; BIR1 in this protein begins at residue 3, 5,

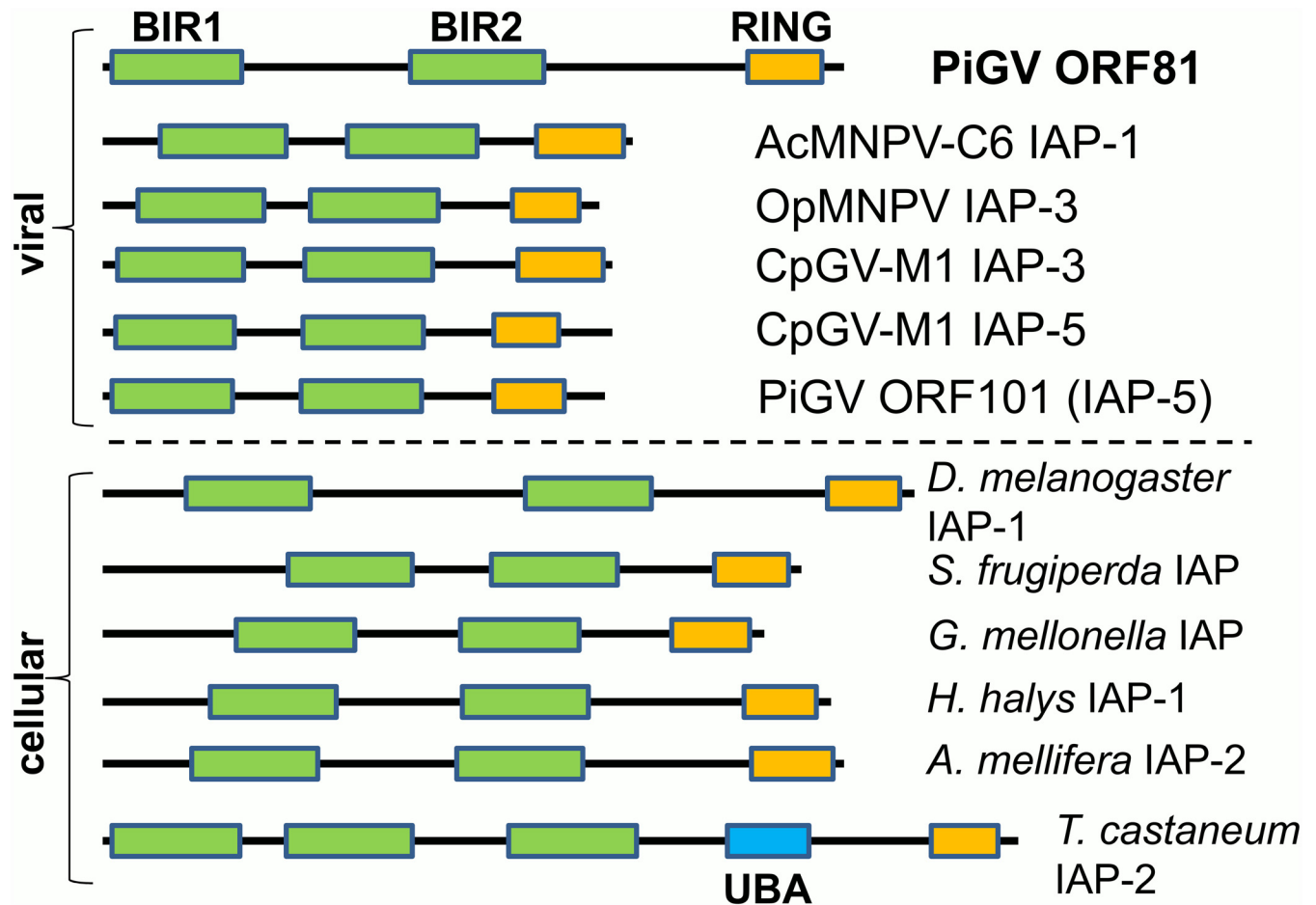


Fig 7. Comparison of PiGV IAPs with representative IAPs from other baculoviruses and insects. A schematic illustration of IAPs from PiGV, selected alphabaculoviruses (AcMNPV-C6, OpMNPV) and betabaculoviruses (CpGV), and insects. Lines representing the IAPs are drawn in proportion to the sizes of the proteins. The BIR domains are shown in green, the RING domain in orange, and the ubiquitin-association domain (UBA) of *T. castaneum* IAP-2 is shown in blue.

doi:10.1371/journal.pone.0160389.g007

or 7 (depending on the specific conserved domain database that is consulted). Also, no sequences similar to the lepidopteran IAP degron, the caspase cleavage site, or the cellular IAP instability motifs identified by Vandergaast et al (2015) [68] are present in PiGV ORF81.

Phylogenetic inference was carried out with a selection of cellular IAPs with two copies of the BIR motif that exhibited significant sequence similarity with the PiGV ORF81 product by blastp, along with baculovirus IAPs of the *iap-1*, *iap-3*, and *iap-5* classes (Fig 8). Many of the basal nodes of this tree did not possess $\geq 50\%$ bootstrap support, but well-supported clades were obtained for the alphabaculovirus IAP-1 and betabaculovirus IAP-5 sequences, as well as sequences from insect orders Diptera, Hymenoptera, Hemiptera, and the moth species of families Noctuidae and Pyralidae. The single termite IAP sequence (from *Zootermopsis nevadensis*) grouped with the hemipteran sequences. While the group I alphabaculovirus IAP-3 sequences were grouped together, the bootstrap support for this clade was not strong. Other IAP-3 sequences from group II alphabaculoviruses and betabaculoviruses did not form a coherent clade, though some IAPs from closely related viruses (e.g. the *Spodoptera* and *Agrotis* spp. NPVs) occurred in terminal and sub-terminal branches that enjoyed good support. The results

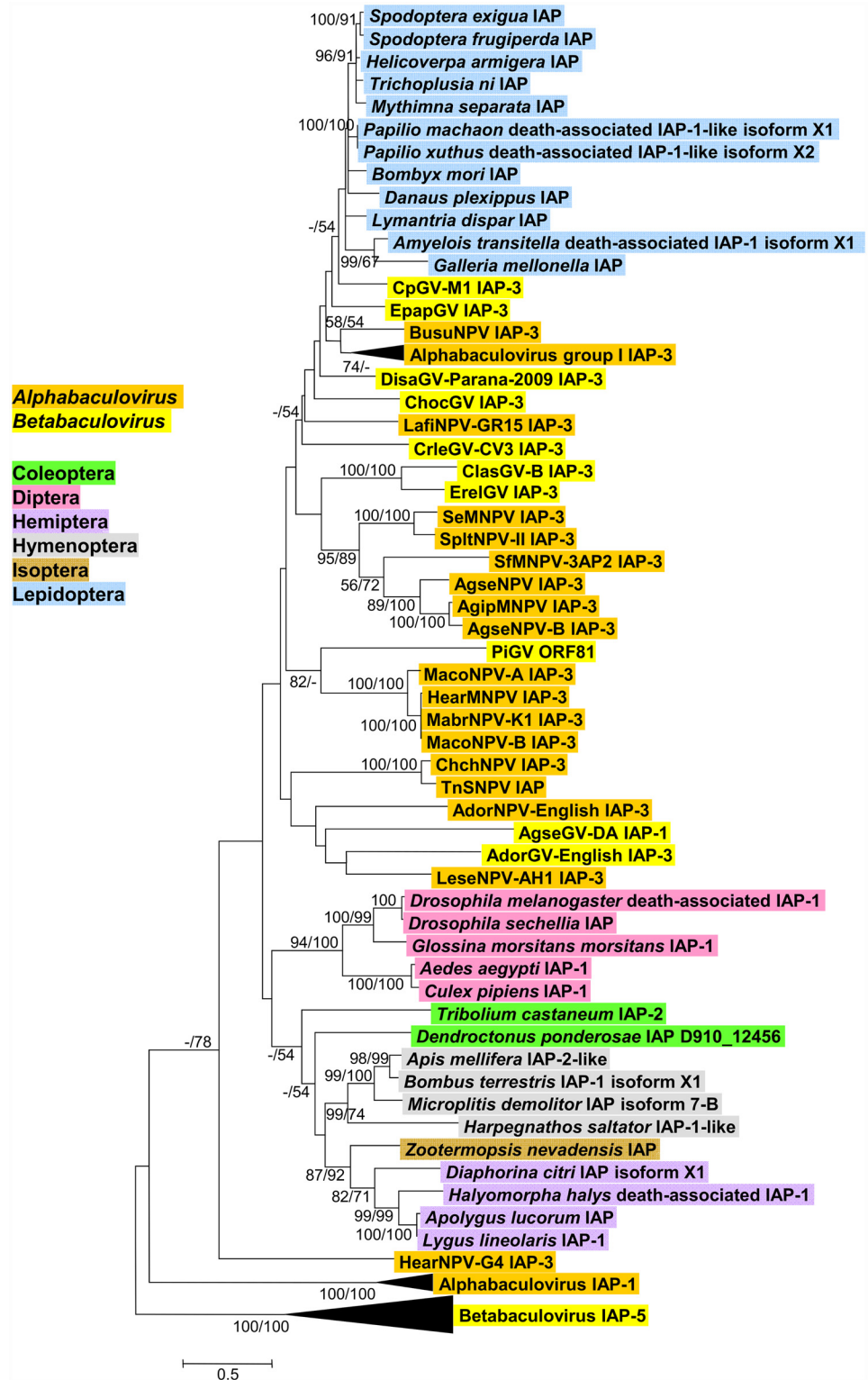


Fig 8. Phylogenetic analysis of viral and cellular IAPs. ML phylogram inferred from the alignment of baculovirus and insect amino acid sequences are shown with bootstrap values (>50%) at interior branches for ME and ML analysis (ME/ML) where they occur. Branches for alphabaculovirus IAP-1, betabaculovirus IAP-5, and group I alphabaculovirus IAP-3 sequences are collapsed, and the nodes for these classes of IAPs are indicated in the tree. The baculovirus genus or insect order for each taxon is indicated with color-coded text background. The virus and insect taxa and their accession numbers are as listed in [S1 Table](#).

doi:10.1371/journal.pone.0160389.g008

of this analysis are similar to a comprehensive phylogenetic analysis of IAPs from many different viral and cellular sources conducted by Thézé and coworkers [58], but different from the phylogenetic analysis carried out by Clem (2015) [67] exclusively with viral sequences in which the IAP-3 sequences all occurred in a single clade. PiGV ORF81 was placed in a group with IAP-3 sequences from *Mamestra* spp. NPVs and the IAP-3 from HearMNPV, which is closely related to the *Mamestra* spp. viruses [69]. Both ME and ML methods placed ORF81 in this clade, although the bootstrap value in the ML tree was only 43%. However, ORF81 and the NPV IAP sequences were separated by long branch lengths.

Phylogenetic analysis by Hughes [70] with a smaller set of baculovirus and host insect IAP sequences placed CpGV IAP-3 and four other NPV IAP-3 sequences in a group with three lepidopteran IAPs with a strong degree of support. While CpGV-M1 IAP-3 was also placed with lepidopteran IAPs in our analysis, the relationships of other viral IAP-3 sequences to the lepidopteran sequences is less clear (Fig 8). In addition to using fewer sequences, the analysis of Hughes also employed alignments of the BIR domain sequences only, which may account for some differences in the results. Nevertheless, it seems clear that the baculovirus IAP-1 and IAP-5 lineages are each due to single acquisition events. It is also possible that the baculovirus IAP-3 genes and the PiGV ORF81 IAP homologue are descended from a single ancient acquisition event followed by extensive sequence divergence, although these sequences do not occur in a single well-supported clade in the IAP phylogeny as is the case for the IAP-1 and IAP-5 sequences.

While some baculovirus IAPs of the IAP-3 group possess demonstrated anti-apoptotic activity, not all baculovirus IAPs have been shown to inhibit apoptosis when tested [66]. The IAPs with proven anti-apoptotic activity do not appear to function by directly binding and inhibiting the effector caspases that trigger apoptosis [71, 72], but instead bind to and stabilize cellular IAPs, which are degraded rapidly in response to baculovirus infection [68, 73]. Since both PiGV IAP-5 and ORF81 have short leader sequences with no degron or instability motifs, it is possible that they would inhibit apoptosis by the same mechanism.

Conclusions

The role of horizontal gene transfer in the evolution and adaptation of organisms has long been recognized [74]. Viruses in particular have been documented as mediators of horizontal gene transfer, and large DNA viruses in particular appear to be mosaics of genes from different sources [75, 76]. In particular, a recent study has provided evidence that baculoviruses may have served to shuttle transposons among different species of host moths [77]. Some environments hypothetically are more conducive to horizontal gene transfer than others. This is likely the case for the Indianmeal moth, *P. interpunctella*. As pests of stored grains and nuts in a wide range of climates and locations, larvae of *P. interpunctella* conceivably could encounter a wide variety of donor gene sources, including microorganisms. One can imagine opportunities for viruses and other microorganisms resident in *P. interpunctella* to acquire genes from a wide taxonomic range of donor genomes. In particular, exposure of *P. interpunctella* to the viruses of other insects that infest grains and nuts could conceivably account for the appearance of genes in the PiGV genome that are present in other distinct lineages of viruses, such as alphabaculoviruses and densoviruses. In support of this hypothesis, an analysis of gene homologues shared by baculoviruses and entomopoxviruses found that ORF *xc138*, originally identified in the XecnGV genome, was apparently transferred directly between entomopoxviruses and granuloviruses on two separate occasions [58]. The sequence of PiGV thus serves to further highlight the concept of viruses as agents for horizontal gene transfer, not only from a virus to a host [78], but to other viruses as well.

Supporting Information

S1 Table. Names, abbreviations, and GenBank accession numbers of taxa used in phylogenetic inference.

(DOCX)

S2 Table. PiGV open reading frames (ORFs) and homologous repeat regions (*hrs*).

(DOCX)

Acknowledgments

The authors would like to thank Jeff Lord (USDA-ARS) for providing a sample of PiGV and William McGaughey and Lee Bulla for information on the source of the PiGV isolate sequenced in this study. Equipment used for purification of the virus and viral DNA isolation was made possible from support by the Arkansas INBRE program, with a grant from the National Institute of General Medical Sciences, (NIGMS), P20 GM103429. Mention of trade names or commercial products in this publication is solely for the purpose of providing specific information and does not imply recommendation or endorsement by the U.S. Department of Agriculture.

Author Contributions

Conceived and designed the experiments: RLH DLR CJF. Performed the experiments: DLR CJF. Analyzed the data: RLH DLR. Contributed reagents/materials/analysis tools: DLR CJF. Wrote the paper: RLH DLR CJF.

References

1. Harrison RL, Hoover K. Baculoviruses and Other Occluded Insect Viruses. In: Vega FE, Kaya HK, editors. *Insect Pathology*, Second Edition. Boston: Academic Press; 2012. p. 73–131.
2. Herniou EA, Arif BM, Becnel JJ, Blissard GW, Bonning B, Harrison RL, et al. Baculoviridae. In: King AMQ, Adams MJ, Carstens EB, Lefkowitz EJ, editors. *Virus Taxonomy: Ninth Report of the International Committee on Taxonomy of Viruses*. Oxford: Elsevier; 2012. p. 163–174.
3. van Oers MM, Pijlman GB, Vlak JM. Thirty years of baculovirus–insect cell protein expression: from dark horse to mainstream technology. *J Gen Virol*. 2015; 96:6–23. doi: [10.1099/vir.0.067108-0](https://doi.org/10.1099/vir.0.067108-0) PMID: [25246703](https://pubmed.ncbi.nlm.nih.gov/25246703/)
4. Winstanley D, Crook NE. Replication of *Cydia pomonella* granulosis virus in cell cultures. *J Gen Virol*. 1993; 74:1599–1609. PMID: [8345351](https://pubmed.ncbi.nlm.nih.gov/8345351/)
5. Arnott HJ, Smith KM. An ultrastructural study of the development of a granulosis virus in the cells of the moth *Plodia interpunctella*. *Journal of Ultrastructure Research*. 1968; 21:251–268.
6. Matthews REF. Classification and nomenclature of viruses. Fourth report of the International Committee on Taxonomy of Viruses. *Intervirology*. 1982; 17:1–199. PMID: [6811498](https://pubmed.ncbi.nlm.nih.gov/6811498/)
7. Hunter DK, Collier SJ, Hoffman DF. Effectiveness of a granulosis virus of the Indian meal moth as a protectant for stored inshell nuts: Preliminary observations. *J Invertebr Pathol*. 1973; 22:481.
8. Hunter DK, Collier SS, Hoffman DF. The effect of a granulosis virus on *Plodia interpunctella* (Hubner) (Lepidoptera: Pyralidae) infestations occurring in stored raisins. *J Stored Prod Res*. 1979; 15:65–69.
9. Vail PV, Hoffman DF, Tebbets JS. Autodissemination of *Plodia interpunctella* (Hubner) (Lepidoptera: Pyralidae) granulosis virus by healthy adults. *J Stored Prod Res*. 1993; 29:71–74.
10. Johnson JA, Vail PV, Brandl DG, Tebbets JS, Valero KA. Integration of nonchemical treatments for control of postharvest pyralid moths (Lepidoptera: Pyralidae) in almonds and raisins. *J Econ Entomol*. 2002; 95(1):190–199. PMID: [11942756](https://pubmed.ncbi.nlm.nih.gov/11942756/)
11. Environmental Protection Agency. Biopesticides Registration Action Document. Indian Meal Moth Granulosis Virus (PC Code 108896), August 18, 2004. Arlington, Virginia: U.S. Environmental Protection Agency, Office of Pesticide Programs. Available: https://www3.epa.gov/pesticides/chem_search/reg_actions/registration/decision_G-110_18-Aug-04.pdf.

12. Tweeten KA, Bulla LA, Consigli RA. Characterization of an extremely basic protein derived from granulosis virus nucleocapsids. *J Virol.* 1980; 33(2):866–876. PMID: [16789190](#)
13. Wilson ME, Consigli RA. Functions of a protein kinase activity associated with purified capsids of the granulosis virus infecting *Plodia interpunctella*. *Virology.* 1985; 143(2):526–535. PMID: [18639856](#)
14. Funk CJ, Consigli RA. Phosphate cycling on the basic protein of *Plodia interpunctella* granulosis virus. *Virology.* 1993; 193(1):396–402. PMID: [8382403](#)
15. Knell RJ, Begon M, Thompson DJ. Transmission of *Plodia interpunctella* granulosis virus does not conform to the mass action model. *J Anim Ecol.* 1998; 67:592–599.
16. Boots M. Cannibalism and the stage-dependent transmission of a viral pathogen of the Indian meal moth, *Plodia interpunctella*. *Ecol Entomol.* 1998; 23:118–122.
17. Burden JP, Griffiths CM, Cory JS, Smith P, Sait SM. Vertical transmission of sublethal granulovirus infection in the Indian meal moth, *Plodia interpunctella*. *Mol Ecol.* 2002; 11(3):547–555. PMID: [11918789](#)
18. Boots M, Meador M. Local interactions select for lower pathogen infectivity. *Science.* 2007; 315(5816):1284–1286. PMID: [17332415](#)
19. Boots M, Begon M. Strain differences in the Indian meal moth, *Plodia interpunctella*, in response to a granulosis virus. *Res Popul Ecol.* 1995; 37:37–42.
20. Meador MA, Boots M. An indirect approach to imply trade-off shapes: population level patterns in resistance suggest a decreasingly costly resistance mechanism in a model insect system. *J Evol Biol.* 2006; 19(2):326–330. PMID: [16599908](#)
21. Boots M. The evolution of resistance to a parasite is determined by resources. *Am Nat.* 2011; 178(2):214–220. doi: [10.1086/660833](#) PMID: [21750385](#)
22. Boots M, Roberts KE. Maternal effects in disease resistance: poor maternal environment increases offspring resistance to an insect virus. *Proc Biol Sci.* 2012; 279(1744):4009–4014. doi: [10.1098/rspb.2012.1073](#) PMID: [22833270](#)
23. McVean RIK, Sait SM, Thompson DJ, Begon M. Dietary stress reduces the susceptibility of *Plodia interpunctella* to infection by a granulovirus. *Biol Control.* 2002; 25:81–84.
24. Bonsall MB, Benmayor R. Multiple infections alter density dependence in host–pathogen interactions. *J Anim Ecol.* 2005; 74:937–945.
25. Saejeng A, Tidbury H, Siva-Jothy MT, Boots M. Examining the relationship between hemolymph phenoloxidase and resistance to a DNA virus, *Plodia interpunctella* granulosis virus (PiGV). *J Insect Physiol.* 2010; 56(9):1232–1236. doi: [10.1016/j.jinsphys.2010.03.025](#) PMID: [20380834](#)
26. Saejeng A, Siva-Jothy MT, Boots M. Low cost antiviral activity of *Plodia interpunctella* haemolymph in vivo demonstrated by dose dependent infection. *J Insect Physiol.* 2011; 57(2):246–250. doi: [10.1016/j.jinsphys.2010.10.005](#) PMID: [21070782](#)
27. Tidbury HJ, Pedersen AB, Boots M. Within and transgenerational immune priming in an insect to a DNA virus. *Proc Biol Sci.* 2011; 278(1707):871–876. doi: [10.1098/rspb.2010.1517](#) PMID: [20861049](#)
28. McGaughey WH. A granulosis virus for Indian meal moth control in stored wheat and corn. *J Econ Entomol.* 1975; 68:346–348.
29. Tweeten KA, Bulla LA Jr., Consigli RA. Supercoiled circular DNA of an insect granulosis virus. *Proc Natl Acad Sci U S A.* 1977; 74(8):3574–3578. PMID: [198791](#)
30. Tweeten KA, Bulla LA Jr., Consigli RA. Isolation and purification of a granulosis virus from infected larvae of the Indian meal moth, *Plodia interpunctella*. *Appl Environ Microbiol.* 1977; 34(3):320–327. PMID: [334076](#)
31. Harrison RL, Lynn DE. Genomic sequence analysis of a nucleopolyhedrovirus isolated from the diamondback moth, *Plutella xylostella*. *Virus Genes.* 2007; 857–873. PMID: [17671835](#)
32. Harrison RL, Keena MA, Rowley DL. Classification, genetic variation and pathogenicity of *Lymantria dispar* nucleopolyhedrovirus isolates from Asia, Europe, and North America. *J Invertebr Pathol.* 2014; 116: 27–35. doi: [10.1016/j.jip.2013.12.005](#) PMID: [24370838](#)
33. Guo F-B, Zhang C-T. ZCURVE_V: a new self-training system for recognizing protein-coding genes in viral and phage genomes. *BMC Bioinformatics.* 2006; 7:9. PMID: [16401352](#)
34. Benson G. Tandem repeats finder: a program to analyze DNA sequences. *Nuc Acids Res.* 1999; 27(2):573–580.
35. Kurtz S, Schleiermacher C. REPuter: fast computation of maximal repeats in complete genomes. *Bioinformatics.* 1999; 15:426–427. PMID: [10366664](#)
36. Hashimoto Y, Hayakawa T, Ueno Y, Fujita T, Sano Y, Matsumoto T. Sequence analysis of the *Plutella xylostella* granulovirus genome. *Virology.* 2000;(275:):358–372.

37. Luque T, Finch R, Crook N, O'Reilly DR, Winstanley D. The complete sequence of the *Cydia pomonella* granulovirus genome. *J Gen Virol.* 2001; 82:2531–2547. PMID: [11562546](#)
38. Zhang BQ, Cheng RL, Wang XF, Zhang CX. The genome of *Pieris rapae* granulovirus. *J Virol.* 2012; 86:9544. doi: [10.1128/JVI.01431-12](#) PMID: [22879615](#)
39. Hu ZH, Arif BM, Jin F, Martens JW, Chen XW, Sun JS, et al. Distinct gene arrangement in the *Buzura suppressaria* single-nucleocapsid nucleopolyhedrovirus genome. *J Gen Virol.* 1998; 79:2841–2851. PMID: [9820162](#)
40. McTaggart SJ, Hannah T, Bridgett S, Garbutt JS, Kaur G, Boots M. Novel insights into the insect transcriptome response to a natural DNA virus. *BMC Genomics.* 2015; 16:310. doi: [10.1186/s12864-015-1499-z](#) PMID: [25924671](#)
41. Garavaglia MJ, Miele SA, Iserte JA, Belaich MN, Ghiringhelli PD. The ac53, ac78, ac101, and ac103 genes are newly discovered core genes in the family *Baculoviridae*. *J Virol.* 2012; 86:12069–12079. doi: [10.1128/JVI.01873-12](#) PMID: [22933288](#)
42. Hall TA. BioEdit: a user-friendly biological sequence alignment editor and analysis program for Windows 95/98/NT. *Nucleic Acids Symp Ser.* 1999; 41:95–98.
43. Tamura K, Stecher G, Peterson D, Filipski A, Kumar S. MEGA6: Molecular Evolutionary Genetics Analysis version 6.0. *Mol Biol Evol.* 2013; 30(12):2725–2729. doi: [10.1093/molbev/mst197](#) PMID: [24132122](#)
44. Stamatakis A, Hoover P, Rougemont J. A rapid bootstrap algorithm for the RAxML Web servers. *Syst Biol.* 2008; 57:758–771. doi: [10.1080/10635150802429642](#) PMID: [18853362](#)
45. Hayakawa T, Ko R, Okano K, Seong SI, Goto C, Maeda S. Sequence analysis of the *Xestia c-nigrum* granulovirus genome. *Virology.* 1999; 262:277–297. PMID: [10502508](#)
46. Harrison RL, Popham HJ. Genomic sequence analysis of a granulovirus isolated from the Old World bollworm, *Helicoverpa armigera*. *Virus Genes.* 2008; 36:565–81. doi: [10.1007/s11262-008-0218-0](#) PMID: [18418706](#)
47. Lange M, Jehle JA. The genome of the *Cryptophlebia leucotreta* granulovirus. *Virology.* 2003; 317:220–236. PMID: [14698662](#)
48. Liang Z, Zhang X, Yin X, Cao S, Xu F. Genomic sequencing and analysis of *Clostera anachoreta* granulovirus. *Arch Virol.* 2011; 156:1185–1198. doi: [10.1007/s00705-011-0977-0](#) PMID: [21442228](#)
49. Hilton S, Winstanley D. The origins of replication of granuloviruses. *Arch Virol.* 2008; 153:1527–1535. doi: [10.1007/s00705-008-0148-0](#) PMID: [18612587](#)
50. Hilton S, Winstanley D. Identification and functional analysis of the origins of DNA replication in the *Cydia pomonella* granulovirus genome. *J Gen Virol.* 2007; 88:1496–1504. PMID: [17412979](#)
51. Miele SA, Garavaglia MJ, Belaich MN, Ghiringhelli PD. Baculovirus: molecular insights on their diversity and conservation. *Int J Evol Biol.* 2011; 2011:379424. doi: [10.4061/2011/379424](#) PMID: [21716740](#)
52. Vanarsdall AL, Pearson MN, Rohrmann GF. Characterization of baculovirus constructs lacking either the Ac 101, Ac 142, or the Ac 144 open reading frame. *Virology.* 2007; 367:187–95. PMID: [17585983](#)
53. Yang ZN, Xu HJ, Park EY, Zhang CX. Characterization of *Bombyx mori* nucleopolyhedrovirus with a deletion of bm118. *Virus Res.* 2008; 135:220–9. doi: [10.1016/j.virusres.2008.03.016](#) PMID: [18462822](#)
54. Hu ZY, Li GH, Li GT, Yao Q, Chen KP. *Bombyx mori bidensovirus*: The type species of the new genus *Bidensovirus* in the new family *Bidnaviridae*. *Chin Sci Bull.* 2013; 58:4528–4532.
55. Ardisson-Araujo DM, de Melo FL, Andrade Mde S, Sihler W, Bao SN, Ribeiro BM, et al. Genome sequence of *Erinnyis ello* granulovirus (ErelGV), a natural cassava hornworm pesticide and the first sequenced sphingid-infecting betabaculovirus. *BMC Genomics.* 2014; 15:856. doi: [10.1186/1471-2164-15-856](#) PMID: [25280947](#)
56. Abd-Alla A, Jousset FX, Li Y, Fediere G, Cousserans F, Bergoin M. NS-3 protein of the *Junonia coenia* densovirus is essential for viral DNA replication in an Ld 652 cell line and *Spodoptera littoralis* larvae. *J Virol.* 2004; 78:790–797. PMID: [14694111](#)
57. Bao YY, Chen LB, Wu WJ, Zhao D, Wang Y, Qin X, et al. Direct interactions between bidensovirus BmDENV-Z proteins and midgut proteins from the virus target *Bombyx mori*. *FEBS J.* 2013; 280:939–949. doi: [10.1111/febs.12088](#) PMID: [23216561](#)
58. Thézé J, Takatsuka J, Nakai M, Arif B, Hernious EA. Gene acquisition convergence between entomopoxviruses and baculoviruses. *Viruses.* 2015; 7, 1960–1974. doi: [10.3390/v7041960](#) PMID: [25871928](#)
59. Ardisson-Araújo DMP, Lima RN, Melo DL, Clem RJ, Huang N, Bao SN, et al. Genome sequence of *Perigonia lusca* single nucleopolyhedrovirus: insights into the evolution of a nucleotide metabolism enzyme in the family *Baculoviridae*. *Sci Rep.* 2016; 6:24612. doi: [10.1038/srep24612](#) PMID: [27273152](#)

60. Tao XY, Choi JY, Kim WJ, An SB, Liu Q, Kim SE, et al. *Autographa californica* multiple nucleopolyhedrovirus ORF11 is essential for budded-virus production and occlusion-derived-virus envelopment. *J Virol*. 2015; 89:373–383. doi: [10.1128/JVI.01742-14](https://doi.org/10.1128/JVI.01742-14) PMID: [25320313](https://pubmed.ncbi.nlm.nih.gov/25320313/)
61. Kuzio J, Pearson MN, Harwood SH, Funk CJ, Evans JT, Slavicek JM, et al. Sequence and analysis of the genome of a baculovirus pathogenic for *Lymantria dispar*. *Virology*. 1999; 253:17–34. PMID: [9887315](https://pubmed.ncbi.nlm.nih.gov/9887315/)
62. Finn RD, Clements J, Arndt W, Miller BL, Wheeler TJ, Schreiber F, et al. HMMER web server: 2015 update. *Nuc Acids Res*. 2015; 43(W1):W30–8.
63. Crook NE, Clem RJ, Miller LK. An apoptosis-inhibiting baculovirus gene with a zinc finger-like motif. *J Virol*. 1993; 67:2168–2174. PMID: [8445726](https://pubmed.ncbi.nlm.nih.gov/8445726/)
64. Birnbaum MJ, Clem RJ, Miller LK. An apoptosis-inhibiting gene from a nuclear polyhedrosis virus encoding a polypeptide with Cys/His sequence motifs. *J Virol*. 1994; 68:2521–2528. PMID: [8139034](https://pubmed.ncbi.nlm.nih.gov/8139034/)
65. Budhidarmo R, Day CL. IAPs: Modular regulators of cell signalling. *Semin Cell Dev Biol*. 2015; 39:80–90. doi: [10.1016/j.semcdb.2014.12.002](https://doi.org/10.1016/j.semcdb.2014.12.002) PMID: [25542341](https://pubmed.ncbi.nlm.nih.gov/25542341/)
66. Estornes Y, Bertrand MJ. IAPs, regulators of innate immunity and inflammation. *Semin Cell Dev Biol*. 2015; 39:106–114. doi: [10.1016/j.semcdb.2014.03.035](https://doi.org/10.1016/j.semcdb.2014.03.035) PMID: [24718315](https://pubmed.ncbi.nlm.nih.gov/24718315/)
67. Clem RJ. Viral IAPs, then and now. *Semin Cell Dev Biol*. 2015; 39:72–79. doi: [10.1016/j.semcdb.2015.01.011](https://doi.org/10.1016/j.semcdb.2015.01.011) PMID: [25652775](https://pubmed.ncbi.nlm.nih.gov/25652775/)
68. Vandergaast R, Mitchell JK, Byers NM, Friesen PD. Insect inhibitor-of-apoptosis (IAP) proteins are negatively regulated by signal-induced N-terminal degrons absent within viral IAP proteins. *J Virol*. 2015; 89:4481–4493. doi: [10.1128/JVI.03659-14](https://doi.org/10.1128/JVI.03659-14) PMID: [25653450](https://pubmed.ncbi.nlm.nih.gov/25653450/)
69. Rowley DL, Popham HJ, Harrison RL. Genetic variation and virulence of nucleopolyhedroviruses isolated worldwide from the heliothine pests *Helicoverpa armigera*, *Helicoverpa zea*, and *Heliothis virescens*. *J Invertebr Pathol*. 2011; 107:112–126. doi: [10.1016/j.jip.2011.03.007](https://doi.org/10.1016/j.jip.2011.03.007) PMID: [21439295](https://pubmed.ncbi.nlm.nih.gov/21439295/)
70. Hughes AL. Evolution of inhibitors of apoptosis in baculoviruses and their insect hosts. *Infect Genet Evol*. 2002; 2:3–10. PMID: [12797996](https://pubmed.ncbi.nlm.nih.gov/12797996/)
71. Wright CW, Means JC, Penabaz T, Clem RJ. The baculovirus anti-apoptotic protein Op- IAP does not inhibit *Drosophila* caspases or apoptosis in *Drosophila* S2 cells and instead sensitizes S2 cells to virus-induced apoptosis. *Virology*. 2005; 335:61–71. PMID: [15823606](https://pubmed.ncbi.nlm.nih.gov/15823606/)
72. Tenev T, Ditzel M, Zachariou A, Meier P. The antiapoptotic activity of insect IAPs requires activation by an evolutionarily conserved mechanism. *Cell Death Differ*. 2007; 14:1191–1201. PMID: [17347664](https://pubmed.ncbi.nlm.nih.gov/17347664/)
73. Byers NM, Vandergaast RL, Friesen PD. Baculovirus inhibitor-of-apoptosis Op-IAP3 blocks apoptosis by interaction with and stabilization of a host insect cellular IAP. *J Virol*. 2015; 90:533–544. doi: [10.1128/JVI.02320-15](https://doi.org/10.1128/JVI.02320-15) PMID: [26491164](https://pubmed.ncbi.nlm.nih.gov/26491164/)
74. Soucy SM, Huang J, Gogarten JP. Horizontal gene transfer: building the web of life. *Nat Rev Genet*. 2015; 16:472–482. doi: [10.1038/nrg3962](https://doi.org/10.1038/nrg3962) PMID: [26184597](https://pubmed.ncbi.nlm.nih.gov/26184597/)
75. Yutin N, Koonin EV. Hidden evolutionary complexity of Nucleo-Cytoplasmic Large DNA viruses of eukaryotes. *Virology*. 2012; 9:161. doi: [10.1186/1743-422X-9-161](https://doi.org/10.1186/1743-422X-9-161) PMID: [22891861](https://pubmed.ncbi.nlm.nih.gov/22891861/)
76. Dennehy JJ. What ecologists can tell virologists. *Annu Rev Microbiol*. 2014; 68:117–135. doi: [10.1146/annurev-micro-091313-103436](https://doi.org/10.1146/annurev-micro-091313-103436) PMID: [24847957](https://pubmed.ncbi.nlm.nih.gov/24847957/)
77. Gilbert C, Chateigner A, Ernenwein L, Barbe V, Bézier A, Herniou EA, et al. Population genomics supports baculoviruses as vectors of horizontal transfer of insect transposons. *Nat Commun* 2014; 5:3348 doi: [10.1038/ncomms4348](https://doi.org/10.1038/ncomms4348) PMID: [24556639](https://pubmed.ncbi.nlm.nih.gov/24556639/)
78. Gasmí L, Boulain H, Gauthier J, Hua-Van A, Musset K, Jakubowska AK, et al. Recurrent domestication by Lepidoptera of genes from their parasites mediated by bracoviruses. *PLoS Genet*. 2015; 11:e1005470. doi: [10.1371/journal.pgen.1005470](https://doi.org/10.1371/journal.pgen.1005470) PMID: [26379286](https://pubmed.ncbi.nlm.nih.gov/26379286/)